Chinese Chemical Letters 33 (2022) 2736–2740

Contents lists available at ScienceDirect

Chinese Chemical Letters

journal homepage: www.elsevier.com/locate/cclet

Halogenated benzothiadiazole-based conjugated polymers as efficient photocatalysts for dye degradation and oxidative coupling of benzylamines

Chu Chu, Yuancheng Qin, Cailing Ni, Jianping Zou*

Key Laboratory of Jiangxi Province for Persistent Pollutants Control and Resources Recycle, Nanchang Hangkong University, Nanchang 330063, China

ARTICLE INFO

Article history:
Received 8 July 2021
Revised 15 August 2021
Accepted 24 August 2021
Available online 31 August 2021

Keywords:
Conjugated polymer
Band gap
Dye degradation
Photocatalysis
Benzylamine oxidation

ABSTRACT

Donor-acceptor (D-A) conjugated polymers are widely used in photovoltaic applications and heterogeneous catalysis due to their tunable building block and pre-designable structures. Here, a series of adjustable Donor-acceptor (D-A) benzothiodiazole-based conjugated polymers were designed and synthesized. The photocatalytic performance could be improved by fine-tuning the chemical structure by halogen substitution (F or Cl). The polymers exhibited excellent optoelectronic properties and were effective photocatalysts for the degradation of RhB and MO dyes, as well as promoting the oxidative coupling of benzylamines. Complete degradation of RhB and MO occurred in 30 min under visible light radiation, while the yield of benzylamine coupling mediated by superoxide anion was as high as 82%. Systematic characterization methods were used to gain insights on the unique photocatalytic performance of the polymers. Our findings provide further insights into the design and synthesis of benzothiadiazole-based conjugated polymers as promising organic photocatalysts for solar energy conversion.

The contributions to human society by synthetic chemicals are undeniable but have simultaneously led to large increases in the release of numerous organic pollutants, including organic dyes, most of which are toxic to aquatic ecosystems due to their low biodegradability and high chemical stability. Therefore, various methods have been developed for the removal and degradation of organic dyes for environmental remediation [1,2]. The covalent organic polymer (COP), a novel type of porous material constructed with a π-conjugated framework, presents a new generation of heterogeneous photocatalyst for solar-energy utilization [3–6]. Theoretically, fast electron-hole recombination is one of the main factors determining photocatalytic efficiency. Therefore, adding electron donor-acceptor (D-A) motifs to a COP photocatalytic system should inhibit the electron-hole recombination rate, thereby greatly improving the photocatalytic activity. In fact, the D-A motif is already known in conjugated polymers such as polymer solar cells (PSCs) [7–9]. In addition, F- and Cl-substituted polymers usually exhibit stronger π-stacking and deeper highest occupied molecular orbital (HOMO) level [6,10]. These features are related to the particular characteristics of fluorine and chlorine atoms, including a smaller van der Waals radius and higher electronegativity.

Herein, a series of 2D isostructural photoactive XBD-BTTs (X = H, F, Cl) COP photocatalysts were synthesized by Knoevenagel condensation under solvothermal conditions. As depicted in Scheme 1, a weak amine-catalyzed Knoevenagel condensation was applied to link BTT with either 4,4-(benzothiadiazole-4,7-diyl)diacetonitrile (HBD-CN), 4,4′-(5,6-difluorobenzo[*c*][1,2,5]thiadiazole-4,7-diyl)diacetonitrile (FBD-CN), or 4,4′-(5,6-dichlorobenzo[*c*] [1,2,5]thiadiazole-4,7-diyl)diacetonitrile (ClBD-CN) to form three different imine-bridged polymers, which were denoted as HBD-BTT, FBD-BTT, and ClBD-BTT, respectively.

There were no distinct peaks observed in the XRD spectrum of XBD-BTTs, suggesting that the samples were non-ordered and amorphous in nature (Fig. S1 in Supporting information). The successful synthesis of each respective XBD-BTT was determined by FT-IR analysis combined with ^{13}C cross-polarization/magic angle spinning solid-state nuclear magnetic resonance (CP/MAS ssNMR) spectroscopy. Compared with BTT, the intensity of the signal at 1692 cm^{-1} in the FT-IR spectrum corresponding to the C=O bond was diminished in XBD-BTTs. In addition, the appearance of distinct peaks at 2225 cm^{-1} in XBD-BTTs corresponding to the cyano group confirmed the high degree of polymerization (Figs. S2-S4 in Supporting information). Due to their similar structures, there

* Corresponding author.
E-mail address: zjp_112@126.com (J. Zou).

https://doi.org/10.1016/j.cclet.2021.08.107
1001-8417/

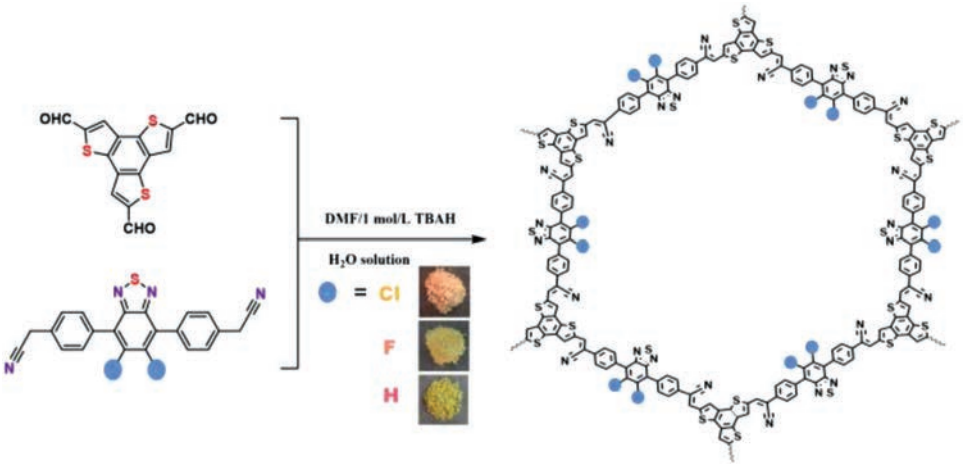

Scheme 1. Synthetic routes of XBD-BTTs under solvothermal conditions.

were no clear differences in the signals of the ^{13}C CPMAS NMR spectra for the various XBD-BTTs polymers. In the formed COPs, we can single out some of the most significant peaks, such as those at ~105 ppm assigned to the cyano groups, those between ~120 and ~140 ppm attributed to olefinic carbons, and the strong resonances at ~127 ppm originating from the aromatic carbons (Fig. S5 in Supporting information).

TGA analysis reflected the higher stabilities at high temperatures of XBD-BTTs polymers, and HBD-BTT could be thermally stable up to 400 °C, while both FBD-BTT and ClBD-BTT maintained more than 80% of their mass up to 500 °C under a nitrogen atmosphere (Fig. S6 in Supporting information). Next, X-ray photoelectron spectroscopy (XPS) was carried out to investigate the chemical states and the types of bonds formed in the XBD-BTTs COPs. As shown in the survey spectra (Fig. S12 in Supporting information), traces of oxygen were detected in three polymers, suggesting that the polymerization reaction did not proceed to completion. By contrast, the XPS peaks at 684.2 eV and 169.0 eV, assigned to F 1s and Cl 2p in FBD-BTT and the ClBD-BTT, respectively, clearly confirmed the presence of halogen ions in XBD-BTTs.

The synthesized COPs exhibited typical type-IV isotherms, as can be determined from the N_2 adsorption-desorption isotherms of XBD-BTTs (X = H, F, Cl). The Brunauer-Emmett-Teller (BET) surface areas of XBD-BTTs (X = H, F, Cl) were calculated as 221.65, 168.21 and 146.07 m^2/g (Fig. S8 in Supporting information), respectively, clearly showing that substitution with a F or Cl halogen atom leads to a much lower surface area. As expected, the pore size distribution calculated based on the nonlocal density functional theory showed that the average pore diameters of XBD-BTTs (X = H, F, Cl) decreased from 12.3 nm in HBD-BTT to 9.86 nm in ClBD-BTT (Fig. S9 in Supporting information).

The surface morphologies of XBD-BTT (X = H, F, Cl) obtained with SEM (Fig. S10 in Supporting information) showed that all polymers formed unevenly sized nanoparticles, while halogenated COPs exhibited much higher degrees of nanoparticle agglomeration. The morphologies of the prepared COPs were further characterized by TEM analysis (Fig. S10). Importantly, the corresponding EDX elemental mappings confirmed the presence of F and Cl in FBD-BTT and ClBD-BTT, respectively (Fig. S11 in Supporting information), further indicating successful halogen incorporation into the corresponding COP. The electronic structures of these polymers were systematically investigated with UV-vis DRS (Fig. 1a), from which it was found that FBD-BTT COPs have a better optical absorption capacity compared to HBD-BTT and ClBD-BTT that could range up to 600 nm, which includes the entire range of the visible spectrum.

Interestingly, halogen incorporation led to a blue-shift in the absorption spectra of the halogenated polymers in comparison to HBD-BTT, confirming the important effect of halogen-doping on the optical properties of XBD-BTTs COPs. Such a blue-shift can be attributed to the intramolecular charge transfer (ICT) caused by the donor-acceptor characteristics inherent in the framework of the halogenated polymers [11].

The optical band gaps of XBD-BTTs (X = H, F, Cl) were calculated as 1.93 eV, 2.02 eV and 2.05 eV, respectively (Fig. 1b). Both FBD-BTT and ClBD-BTT show slight increases in the band gap, an effect which is slightly higher in the chlorinated polymer, consistent with similar findings in the literature [11,12]. Overall, the ClBD-BTT COP exhibited the highest optical band gap among these polymers (2.05 eV). The increase in the band gap of halogenated XBD-BTTs polymers may be due to the presence of the X 2p and O 2p orbitals and the resulting energy sub-levels [13,14], a phenomenon that was most pronounced in ClBD-BTT, suggesting that the effect may be dependent on the electronegativity of the halogen incorporated in the polymer.

The VB potentials (EVB) of XBD-BTTs (X = H, F, Cl) polymers were approximately determined by the XPS VB spectra as 1.08, 1.19 and 1.22 eV, respectively (Fig. S12 in Supporting information), while the energies of the conduction band minimum (ECB) were determined to be −0.85, −0.83, and −0.83 eV, respectively. Hence, the ECBs of all three polymers were greater than the potential of $O_2/O_2^{\bullet-}$ (–0.33 eV).

The Mott-Schottky plot indicated that the XBD-BTTs polymers acted as n-type semiconductors. The calculated flat-band potentials of XBD-BTTs (X = H, F, Cl) were −0.94 V, −0.90 V and −0.88 V, respectively, versus NHE at pH 7 (Fig. S13 in Supporting information), which are quite close to the potential at the bottom of the conduction band (CB). In addition, XBD-BTT polymers were expected to be able to reduce O_2 to $O_2^{\bullet-}$ upon photoexcitation. The general trend measured by Gaussian is also observed in the calculations: the HOMO level gets deeper and deeper when going from HBD-BTT to FBD-BTT and ClBD-BTT. The band gap trend calculated by HOMO and LUMO is with all the UV−vis measurements (Table S1 in Supporting information).

The origins of the enhanced photocatalytic performances of these halogenated polymers were investigated with transient photocurrent measurements and electrochemical impedance spectroscopy (EIS) to evaluate the photocurrent response and the electrical conductivity of the photocatalysts. Compared with HBD-BTT, the instantaneous photocurrents of FBD-BTT and ClBD-BTT were significantly enhanced, indicating that these photocatalysts exhibited higher photo current responses (Fig. 1c), suggesting that their

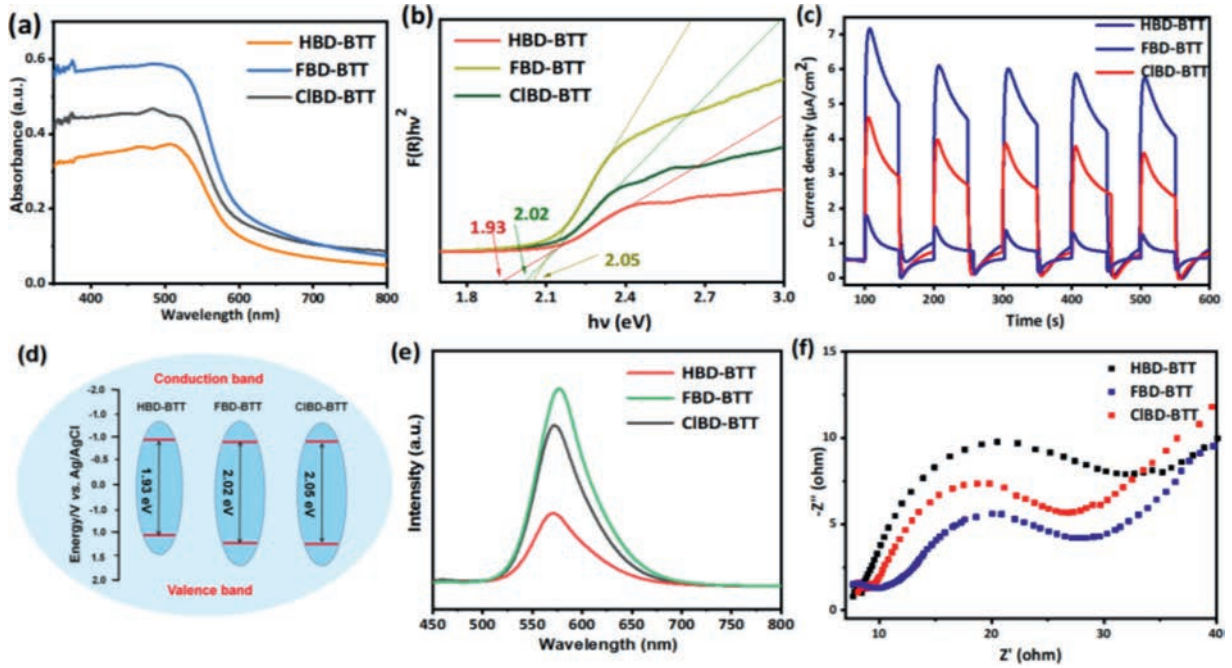

Fig. 1. (a) UV-DRS spectra of XBD-BTTs (b) Tauc plot of the XBD-BTTs. (c) EIS of the XBD-BTTs. (d) Band energy diagram of XBD-BTTs. (e) TR-PL spectra of XBD-BTTs. (f) Transient photocurrent of XBD-BTTs.

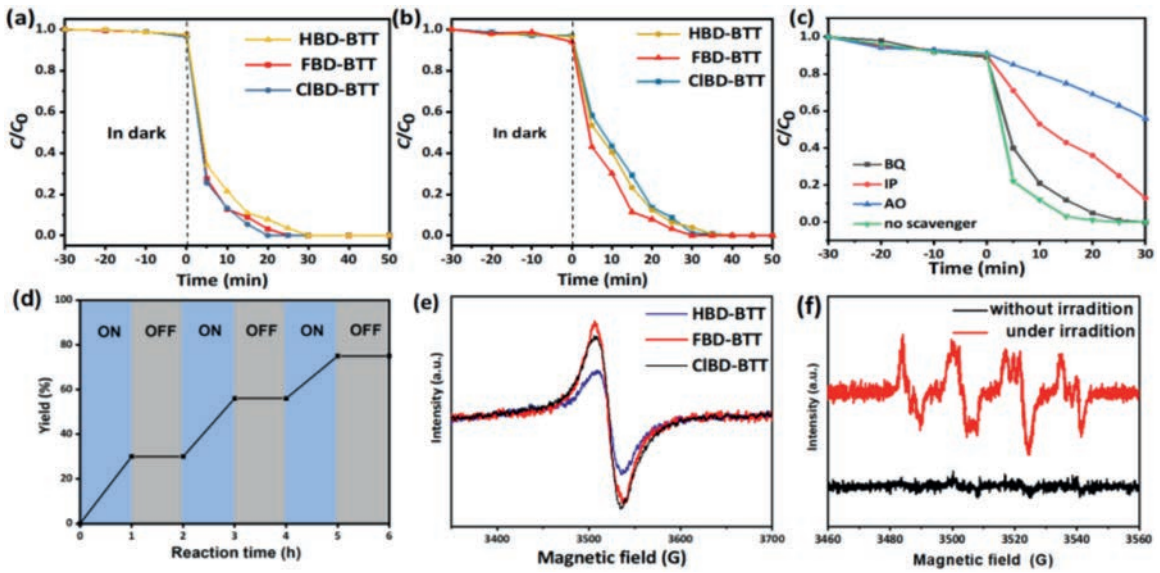

Fig. 2. Photocatalytic degradation of (a) RhB and (b) MO of XBD-BTTs. (c) Effect of different scavengers on the degradation of RhB over ClBD-BTT with 30 min of visible-light irradiation. (d) Photodynamic monitoring of the ClBD-BTT. (e) EPR spectra of XBD-BTTs; (f) DMPO-O_2^- –spin-trapping EPR spectra of the ClBD-BTT.

charge recombination rates were lower while showing more efficient charge transfer. The energy bands of XBD-BTTs are shown in Fig. 1d. Additionally, the dramatic reduction of the arc radius suggested that the reduced resistance was due to the increased charge density in the FBD-BTT and ClBD-BTT polymers, which manifested in a faster interfacial charge transfer in the photocatalytic process (Fig. 1f). Photoluminescence (PL) spectroscopy was employed to further explore the charge migration dynamics of XBD-BTT polymers. A single peak was observed in each polymer very close to 573 nm with remarkably different intensities, and the halogenated polymers ClBD-BTT and FBD-BTT exhibited the strongest fluorescence intensities (Fig. 1e). This showed that in the presence of F-ions and Cl-ions, the recombination efficiency of the carriers could be improved. In halogen (X) substituted polymers, the high electronegativity of X reduces electron density around the C-S bond, and thus generates a greater number of electron vacancies. Subsequent X substitution induced the vacancies to capture photogenerated electrons and accelerate the recombination.

In order to evaluate the practical utility of these novel COPs, we evaluated the photocatalytic activity of XBD-BTTs polymers in the degradation of RhB and MO dyes. After treatment under dark conditions to establish the appropriate adsorption-desorption equilibrium between the dye and the photocatalyst, all XBD-BTTs polymers could completely degrade RhB and MO in a shorter period of time under visible light. The ClBD-BTT polymer had the highest photocatalytic activity for RhB degradation, accomplished within 20 min, while HBD-BTT and FBD-BTT degraded the same dye in 30 and 25 min, respectively (Fig. 2a and Fig. S14 in Supporting

information). Photo-degradation experiments under visible light of MO dye in aqueous solution (10 ppm), and under otherwise similar conditions (same concentration of XBD-BTTs), showed that MO dye was more difficult to degrade (Fig. 2b and Fig. S15 in Supporting information). The HBD-BTT polymer had the lowest photocatalytic activity against RhB, degrading the dye in 40 min, while the degradation time in both FBD-BTT and ClBD-BTT was 30 min.

The results illustrated that the dye degradation reaction with XBT-BTTs all belonged to the first-order reaction (Fig. S16 in Supporting information), and that the photocatalysts all exhibited great cyclicity, with only a slight reduction in the relative activity after five runs (Fig. S17 in Supporting information).

In order to investigate the active species during the photocatalytic degradation of RhB, a series of radical trapping experiments were conducted by adding different scavengers and ClBD-BTT as the photocatalyst (Fig. 2c). The degradation of the dyes was greatly hindered by the addition of the superoxide radical scavenger *p*-benzoquinone (BQ), while adding isopropanol (IP) led to the degradation of a small quantity of RhB. However, there was only a slight decrease in the RhB degradation efficiency with ClBD-BTT as a photocatalyst after addition of ammonium oxalate (AO). Hence, the photo degradation of dyes appears to be primarily driven by the presence of superoxide radical anion ($O_2^{\bullet-}$) and holes (H^+) rather than hydroxyl radicals ($^{\bullet}OH$).

The photocatalytic aerobic oxidation of primary amines to imines is an environmentally benign alternative for traditional oxidative coupling, which typically requires harsher conditions. Hence, considering the photoelectronic properties of XBD-BTT polymers, we evaluated their photocatalytic activity to drive the oxidative coupling reaction of benzylamines under visible light.

First, benzylamine and two of its derivatives containing either an electron-withdrawing group (–F) or an electron-donating group ($–OCH_3$) were investigated, and the results are listed in Table 1. As expected, the reaction catalyzed with ClBD-BTT under the same conditions achieved significantly higher conversions than HBD-BTT and FBD-BTT, with rates of 82%, 67%, and 73%, respectively. The ClBD-BTT polymer exhibited a stronger EPR signal than both HBD-BTT and FBD-BTT (Fig. 2e). The ClBD-BTT polymer exhibited nice recyclability and stability with little change in the relative activity after five runs (Figs. S18 and S19 in Supporting information), and at this stage the peaks in the FT-IR spectrum (Fig. S20 in Supporting information) of the photocatalyst were slightly attenuated, showing that the catalyst structure or framework had been slightly degraded.

To further explain the reaction mechanism, we conducted several control experiments, as shown in Table 1. None of the final products were observed in the absence of light, ClBD-BTT as a catalyst, or O_2 (Table 1, entries 4, 5, and 6, respectively), while with benzoquinone as superoxide scavenger the conversion was only 7% (entry 8). In addition, we conducted a kinetic test with intermittent light in order to confirm the critical role of oxygen in the photocatalytic reaction. The experimental results showed that conversion of the reactant to product only took place under light radiation, showing that light energy is required for the reaction to proceed (Fig. 2d). To gain more insight into the radical mechanism of the reaction, either $Edta_2Na$ hole or benzoquinone radical scavengers were added in separate reactions, which resulted in a sharp decrease in the yields of imine to only 10% and 7%, respectively (entries 7 and 8, Table 1). Next, when the reaction was tested in the presence of isopropanol as a hydroxyl radical ($^{\bullet}OH$) scavenger, a conversion of 79% was observed (entry 9). These results indicated that $O_2^{\bullet-}$ radicals and holes could play significant roles in the catalytic process.

Electron paramagnetic resonance (EPR) spectroscopy shed further light on the reaction mechanism. After irradiating a reaction mixture containing ClBD-BTT and 5,5-dimethyl-1-pyrroline *N*-oxide (DMPO) for 10 min, clear EPR signals were present, indicating the formation of $O_2^{\bullet-}$ radicals spin trapped by DMPO (Fig. 2f).

Table 1
Photocatalytic oxidative coupling reactions of various amines by XBD-BTTs.[a]

Entry	Substrate	Product	Yield (%)[b]
1	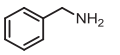	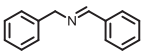	67[c] 73[d] 82[e]
2	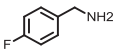	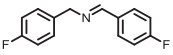	49[c] 51[d] 60[e]
3	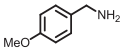	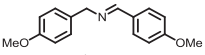	26[c] 17[d] 37[e]
4[f]	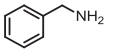	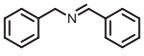	none
5[g]	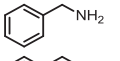	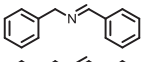	none
6[h]	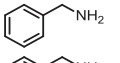	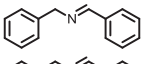	none
7[i]	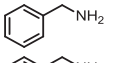	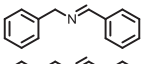	10
8[j]	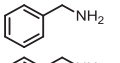	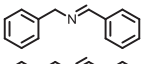	7
9[k]	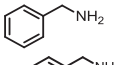	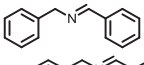	79
10	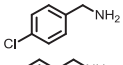	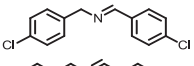	53
11	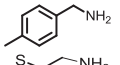	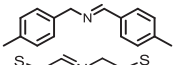	35
12	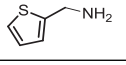	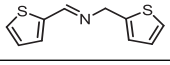	14

[a] Reaction conditions: 2 mmol substrate, 10 mg of catalyst, 5 mL of CH_3CN, 6 h, 30 °C, 1 atm of O_2, 300 W XE LAMP. Entries 4-12 were catalyzed by ClBD-BTT.
[b] Yield data obtained by ^1H NMR.
[c] Catalyst: HBD-BTT.
[d] Catalyst: FBD-BTT.
[e] Catalyst: ClBD-BTT.
[f] In dark, 24 h.
[g] No ClBD-BTT, but under light, 6 h.
[h] No O_2, with FBD-BTT, under light, 6 h.
[i] $Edta_2Na$ as hole scavenger.
[j] Benzoquinone as superoxide scavenger.
[k] Isopropanol as $^{\bullet}OH$ scavenger.

To further demonstrate the general applicability of ClBD-BTT as a photocatalyst, different benzylamine substrates were used in the oxidative coupling reaction (Table 1). Benzylamine analogues with larger groups in the *para*-position had lower yields ($CH_3O–$ and $CH_3–$ substitution, entries 12 and 13), while the highest conversions were observed with the very small *para*-halogen substituted analogs (F– and Cl–, entries 11 and 12). Presumably, the observed steric effect could be due in part to steric requirements for entrance of the substrate molecule into the pores of the photocatalyst pores of the photocatalyst. Therefore, building on our test results, we propose a mechanism for the photocatalytic oxidation of benzylamine with ClBD-BTT (Scheme S4 in Supporting information).

In summary, we successfully developed a series of efficient XBD-BTTs (X = H, F, Cl) photocatalysts based on a core benzothiadiazole structural motif. We observed that halogen substituted polymers not only exhibited enhanced photocatalytic activity, but also showed enlarged optical band gaps. Serving as a photocatalyst for the degradation of organic dyes and visible-light-driven oxidative coupling of amines, ClBD-BTT showed remarkable catalytic performance. Thus, our study provides a new method and strategy for the design and tailoring of high-performance organic photocatalysts.

Declaration of competing interest

The authors declare that they have no known competing financial interests or personal relationships that could have appeared to influence the work reported in this paper .

Acknowledgments

The work was financially supported by National Natural Science Foundation of China (No. 52173099), the Science and Technology Department of Jiangxi Province (No. 20192BBEL50025), Nanchang Hangkong University (No. EA201902288) and the Special Fund for Graduate Innovation (No. YC2020-011).

Supplementary materials

Supplementary material associated with this article can be found, in the online version, at doi:10.1016/j.cclet.2021.08.107.

References

[1] Y.B. Zhou, J. Lu, Y. Zhou, Y.D. Liu, Environ. Pollut. 252 (2019) 352–365.
[2] M.A. Islam, I. Ali, S.M.A. Karim, et al., J. Water Process. Eng. 32 (2019) 100911.
[3] K. Rakstys, S. Paek, P. Gao, et al., J. Mater. Chem. A 5 (2017) 7811–7815.
[4] L. An, Y. Huang, X. Wang, et al., Polymers 12 (2020) 504.
[5] X.B. Wen, A. Nowak-Krol, O. Nagler, et al., Angew. Chem. Int. Ed. 58 (2019) 13051–13055.
[6] Z.M. Hu, H. Chen, J.F. Qu, et al., ACS Energy Lett. 2 (2017) 753–758.
[7] A.W. He, Y.C. Qin, W.L. Dai, X.B. Luo, Dyes Pigments 162 (2019) 671–679.
[8] Y.C. Qin, S.Q. Liu, H.H. Gu, W.L. Dai, X.B. Luo, Sol. Energy 166 (2018) 450–457.
[9] Y.C. Qin, Y.Y. Cheng, L.Y. Jiang, et al., ACS Sustainable Chem. Eng. 3 (2015) 637–644.
[10] T. Olla, O.A. Ibraikulov, S. Ferry, O. Boyron, et al., Macromolecules 52 (2019) 8006–8016.
[11] S. Bi, P. Thiruvengadam, S. Wei, et al., J. Am. Chem. Soc. 142 (2020) 11893–11900.
[12] W. Chen, L. Wang, D. Mo, et al., Angew. Chem. Int. Ed. 59 (2020) 16902–16909.
[13] Z. Khazaee, A.H.C. Khavar, A.R. Mahjoub, et al., Sol. Energy 196 (2020) 567–581.
[14] P.P. Filippatos, A. Soultati, N. Kelaidis, et al., Sci. Rep. 11 (2021) 5700.